

U. KAISER*, TH. KUPS, A. FISSEL, W. RICHTER

Institut für Festkörperphysik, Friedrich Schiller Universität, Jena 07743, Germany

Structure of SiC-Quantum Wells Studied by TEM and CBED

Multi-quantum well structures of 3C/4H-SiC polytypes grown either on stepped or on on-axis hexagonal SiC by molecular beam epitaxy have been investigated by conventional and high resolution TEM. The 3C-SiC layers were nearly free of defects and the interface between different polytypes was abrupt. For the 3C-SiC layers the strain state and the lattice parameters have been investigated to a high accuracy by convergent beam electron diffraction (CBED).

Keywords: SiC, heterostructures, TEM, convergent beam electron diffraction, lattice parameter

(Received March 12, 2002; Accepted March 26, 2002)

Introduction

The preparation of semiconductor heterostructures has been focused mostly on systems consisting of different chemical materials as for instance GaAs/AlAs. However new developments consider a theoretical [BECHSTEDT] as well as practical [Fissel (a), FISSEL (b)] approach to heterostructures composed of SiC. SiC is a polytypic material and has the advantage over most other semiconductors that heterostructures and superlattices can be built from one and the same chemical compound by using a combination of the cubic (zincblende, F-43m) and another non-cubic polytypes, i.e., hexagonal 4H-SiC (P₆mc). Recently the successful growth of multi-quantum well structures of SiC consisting of 3C-SiC wells and hexagonal SiC barriers is demonstrated [FISSEL (c)]. However the presence of defects on an atomic scale can be detrimental to the properties of the devices. They can give rise to local variations of the lattice parameter and strain state of the lattice [KAISER (a)]. Lattice parameters can be determined to high accuracy by X-ray diffraction (XRD) [KRÄUBLICH], however this method averages over the whole crystal volume and therefore cannot be helpful when local information from tiny specimen regions is required. Convergent beam electron diffraction (CBED) is the method of choice to measure local variations of crystal lattice parameters and due to the high sensitivity of Higher Order Laue Zone (HOLZ) lines appearing in the CBED patterns at definite incident electron energy, the accuracy of the method can be very high [ZUO (a)], [KAISER (a)]. To determine lattice parameters, experiments and simulations have to be compared. As nowadays computer time limitations for Bloch wave calculations are no longer a severe factor, full dynamical calculations should be preferably performed. To compare experimental and calculated CBED patterns, different methods have been successfully applied so far. That are: fitting the whole CBED pattern [ZOU (a)], fitting ratios of areas of triangles defined by particular HOLZ lines [ROZEVELD],

* corresponding author: kaiser@pinet.uni-jena.de

[WITTMAN], determine distances between HOLZ line intersections [KRAEMER (a), (b)], or ratios of distances between HOLZ line intersections [WAKAYAMA], [KAISER (a)], [YONEMURA]. These quantities had been determined differently, either using image processing programs [WAKAYAMA], linear regression on the positions of line maxima [WITTMAN], or the Hough transformation [HOUGH]. For the latter method integrated data from the whole lines are used which allow achieving sub-pixel accuracy routinely [KRAEMER (b)].

In this paper we investigate multi-quantum well structures of SiC and determine the lattice parameters of thin cubic SiC stripes embedded in 4H-SiC using full dynamical calculations and a fitting procedure based on the Hough transformation.

Methods

SiC multi-quantum well growth

The growth experiments were performed by solid-source molecular beam epitaxy either in the step flow growth mode on stepped hexagonal SiC substrates [FISSEL (b)] or on hexagonal on-axis SiC substrates. The growth of the hexagonal (4H- or 6H-SiC) and 3C-SiC growth was realized adjusting C-rich and Si-rich vapour pressure conditions on the growing surface, respectively [FISSEL (b)], [FISSEL (d)]. For more details on the growth process see [FISSEL (e)].

Transmission electron microscopy, simulations and fitting procedure

Cross-sectional samples were prepared for TEM experiments using standard techniques including mechanical polishing, dimpling and low-angle Ar-ion milling. Microscopy was carried out using a JEOL 3010 TEM equipped with a LaB₆ cathode, operated at 300kV for the conventional and high-resolution investigations and at 100kV for the CBED investigations. For the kinematical calculations of Kikuchi-line maps we used the program of Morniroli [MORNIROLI]. The exact accelerating voltage of the microscope has been calibrated from CBED patterns obtained at [0001] zone axis incidence of high quality bulk 6H-SiC specimens. The lattice parameters of the 6H-SiC wafer of $a = 0.308129$ nm and $c = 1.511975$ nm have been measured to high accuracy by X-ray analysis [KRÄUBLICH]. For the lattice parameter determination of the 3C-SiC stripe CBED pattern obtained at [661] incidence have been used. For the dynamic calculations of CBED patterns the program of Tsuda and Tanaka [TSUDA] has been applied which uses atomic scattering factors calculated by Doyle and Turner [DOYLE]. The input values were: Si and C atom co-ordinates of 6H-SiC (P₆,mc), 3C-SiC (F $\bar{4}$ 3m) and 3C-SiC(R3m), respectively; Debye -Waller factors: for 6H-SiC[0001] $B_{Si} = 0.50A^2$, $B_C = 0.50A^2$ and for 3C-SiC[661] (F $\bar{4}$ 3m and R3m) $B_{Si} = 0.20A^2$, $B_C = 0.25A^2$; Laue zones: for 6H-SiC: 1st to 2nd order, for 3C-SiC and rhombohedral SiC: 1st to 9th order; number of beams: at 6H-SiC [0001] zone: 265, at 3C-SiC [661] (F $\bar{4}$ 3m) zone: 89 and at the rhombohedral SiC [661] (R3m) zone: 332; number of pixels: 301 (for all). Experimental and simulated patterns have been compared using an automated fitting procedure, based on the Hough transformation, where the geometrical error of the measurement is automatically determined [CHUVILIN]. Ratios of distances between HOLZ

line intersections have been used moving in different directions with small variations of the lattice parameter (or accelerating voltage) [KAISER (a)]. For the actual measurements, an accuracy of at least 0.1% was achieved.

Results and discussion

The specimens in the direct space

Fig. 1 shows bright-field and high-resolution images in cross-sectional view of a 4H-3C-SiC multi-quantum well structure grown in the step-controlled growth mode. In Fig. 1a, specimen tilt of about 10° off [11-20] zone towards [0001] was chosen to enhance contrast differences between the cubic and hexagonal SiC polytype.

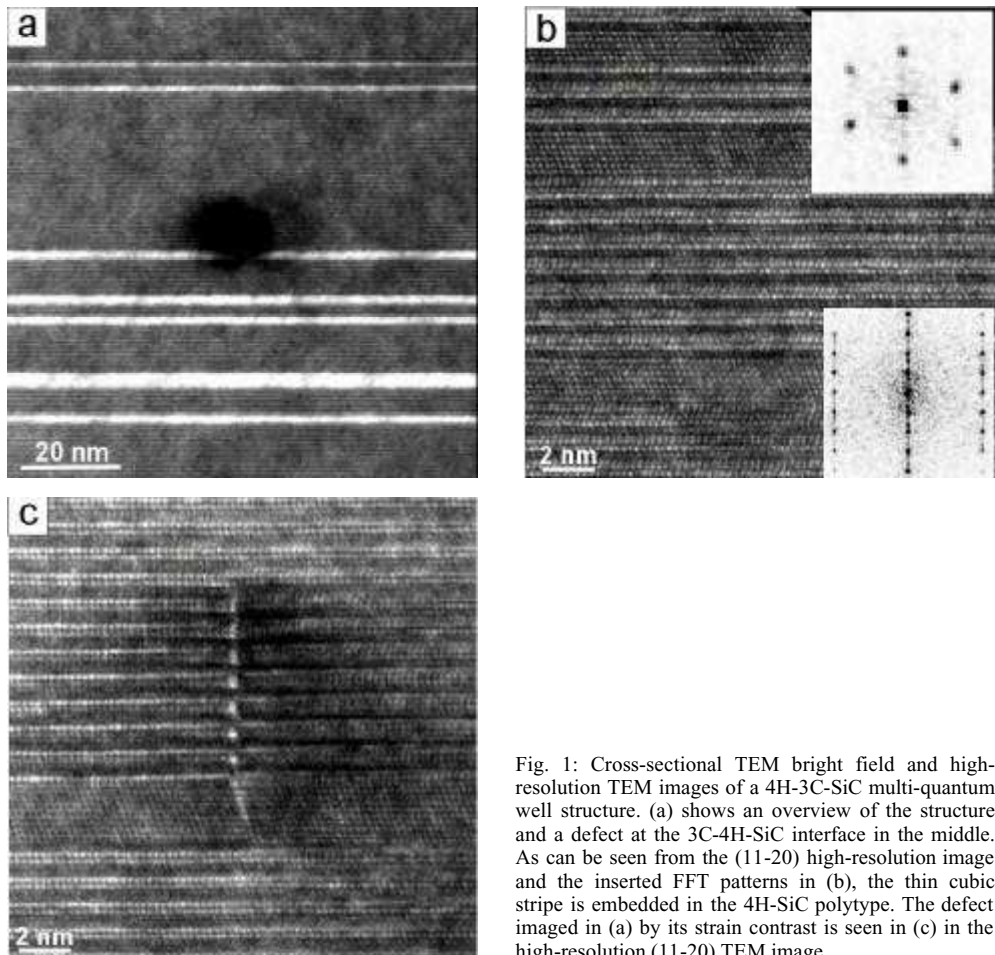


Fig. 1: Cross-sectional TEM bright field and high-resolution TEM images of a 4H-3C-SiC multi-quantum well structure. (a) shows an overview of the structure and a defect at the 3C-4H-SiC interface in the middle. As can be seen from the (11-20) high-resolution image and the inserted FFT patterns in (b), the thin cubic stripe is embedded in the 4H-SiC polytype. The defect imaged in (a) by its strain contrast is seen in (c) in the high-resolution (11-20) TEM image.

The thin bright stripes correspond to the cubic phase. The number and the width of the 3C stripes depend on the step height and the corresponding terrace width of the off-axis angle of the 4H-SiC substrate. As can be seen from the 11-20 high-resolution image in Fig. 1b, the

thin cubic stripe (see the FFT inserted on the upper right corner) is embedded in the 4H-SiC polytype (see the FFT inserted in the lower right corner, obtained from the whole image). The cubic lamellae have an average thickness of about 2nm. Occasionally defects are formed, visualized by strain contrast in bright field as seen in Fig. 1a. The defect nature was clarified by (11-20) high-resolution imaging as a (01-10) grain boundary plane inside the hexagonal stripe, originating from a stacking fault in the cubic stripe (see in Fig. 1c). It should be noted that, except irregularities in the stacking in the surrounding of a defect, only the 4H-SiC but not the 6H-SiC polytype has been found. This is confirm with the fact that first wire-like 3C-SiC nuclei were nucleated selectively on some larger terraces of the 4H-SiC(0001) substrates at low T (<1500 K). Subsequent, the 3C wires and the surrounding 4H-SiC substrate material was grown via step-flow at higher temperature (T = 1600 K) [FISSEL (b)].

Fig. 2 shows heterostructures grown on an on-axis substrate where one polytype has been grown after the other. The bright/dark contrast changes of the hexagonal polytype can be easily distinguished from the homogeneous contrast of the cubic polytype. Generally the layers are grown perfectly on each other.

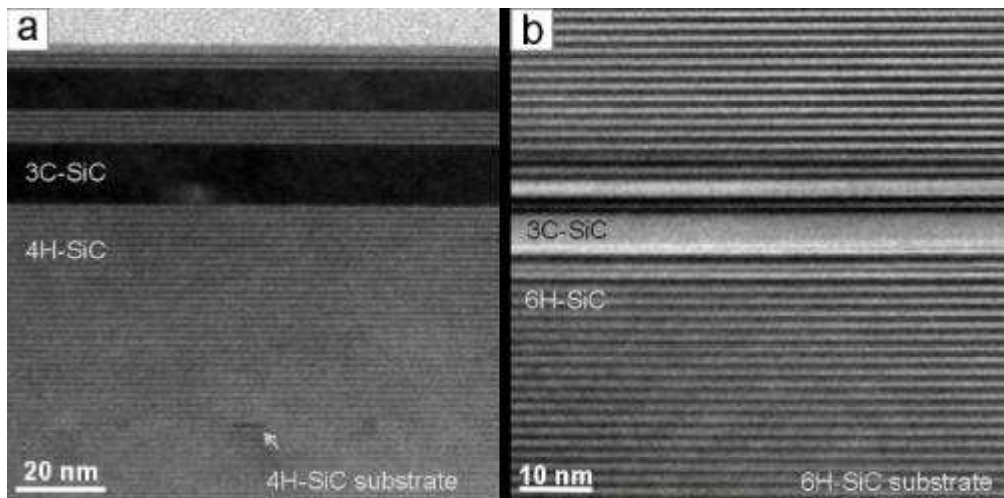


Fig. 2: Bright-field images of heterostructures grown on an on-axis (a) 4H-SiC and (b) 6H-SiC substrate. The 4H-SiC substrate / 4H-SiC layer interface is indicated by small strain contrast (as arrowed).

In Fig. 2a and b image of a 4H/3C stacking on 4H-SiC and 6H/3C stacking on 6H-SiC substrates, respectively are presented. In Fig. 2a, the 4H-SiC substrate / 4H-SiC layer interface is indicated by weak strain contrast (as arrowed), what is likely due to the high doping level of the substrate. It was confirmed by TEM on different multi-quantum well structures grown on on-axis substrates that surprisingly only 4H/3C heterostructures grow on 4H-SiC substrates and 6H/3C on 6H-substrates. As the a-lattice parameter between hexagonal polytypes differs (however slightly, see Table 1) and the cubic polytype is expected to grown pseudomorphically on hexagonal SiC, it follows that the cubic SiC is expected to be strained and moreover slightly differently strained on different hexagonal

polytypes. In this case, there is a strain contribution to the nucleation energy of the polytype grown on 3C [FISSEL (d)]. This might be the reason for the preferential growth of 4H on 3C/4H-SiC and 6H on 3C/6H-SiC, respectively.

Table 1: Lattice parameters of cubic and hexagonal SiC. The cubic values were transferred into the hexagonal value by using the following relationship: $a_{hex} = \sin(\alpha/2) \cdot a_{cub}$ (α rhombohedral angle).

	cubic	hexagonal
table values		$a_{4H-SiC} = 0.30805 \text{ nm}$
SiC (a_{cub}, a_{hex})	$a_{cub} = 0.43596 \text{ nm}$	$c_{4H-SiC} = 1.08481 \text{ nm}$
[KRÄUBLICH]	$a_{hex} = 0.30828 \text{ nm}$	$a_{6H-SiC} = 0.30813 \text{ nm}$
		$c_{6H-SiC} = 1.51198 \text{ nm}$

To determine the strain state of a cubic quantum well grown on 4H-SiC, CBED was applied. The 3C SiC-layers in Fig. 1a are too small for the electron beam of about 6nm to be focused only on the stripe. Therefore the strain state of a 20nm wide cubic stripe within 4H-SiC was analysed by CBED.

Determination of the actual accelerating voltage

Fig. 3a shows an experimental [0001] CBED pattern of the 4H-SiC standard specimen used for the determination of the actual high tension of the microscope.

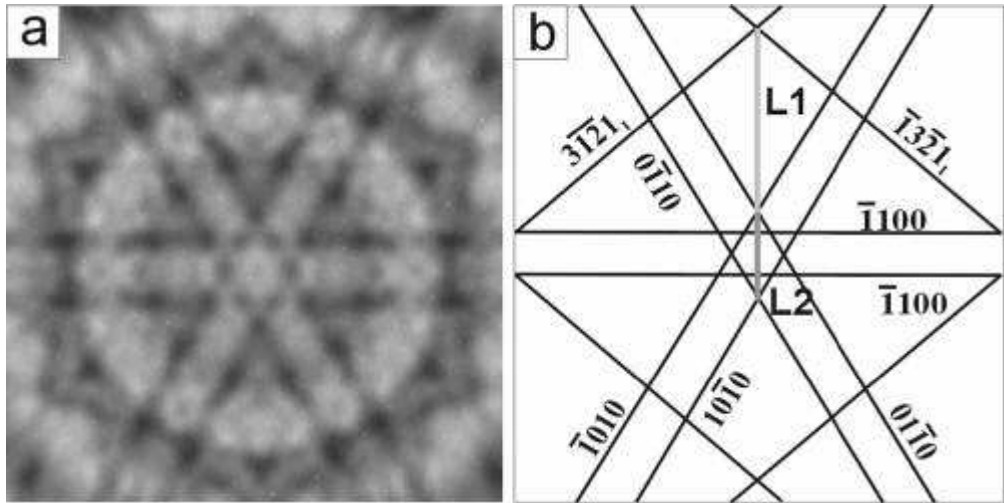


Fig. 3: (a) Experimental CBED pattern of 6H-SiC [0001] at about 100kV and (b) the indexed pattern with the ratio $R = L1/L2$, used for the exact high tension determination.

The lattice parameters of this high quality SiC material were determined to high accuracy by XRD [KRÄUBLICH] (see Table 1). Fig. 3b shows the scheme of the HOLZ-lines taken from Fig. 3a together with the ratio of the line distances used for the accelerating voltage determination. Although all HOLZ lines, which provide these distances, belong to the first order Laue zone, they are very sensitive to small changes of the accelerating voltage as is demonstrated by the dynamically calculated patterns in Fig. 4.

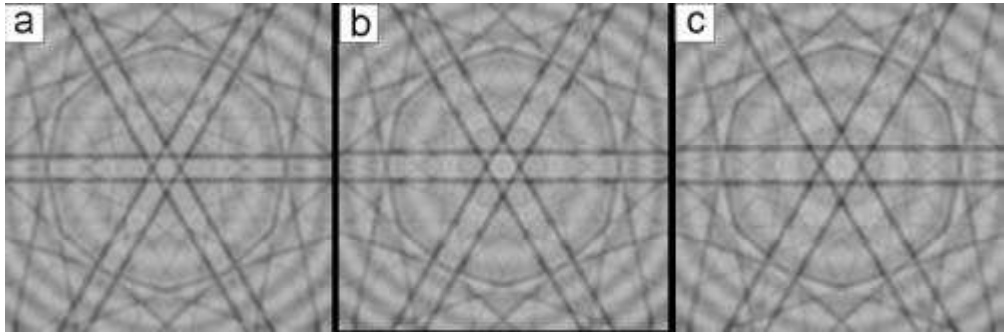


Fig. 4: Dynamical simulated CBED patterns of 6H-SiC [0001] for different voltages: (a) 99.9kV, (b) 100.3kV, (c) 100.7kV.

It should be noted that to obtain an accuracy of 0.1% in the lattice parameter, the high voltage has to be determined with an accuracy of 0.2%.

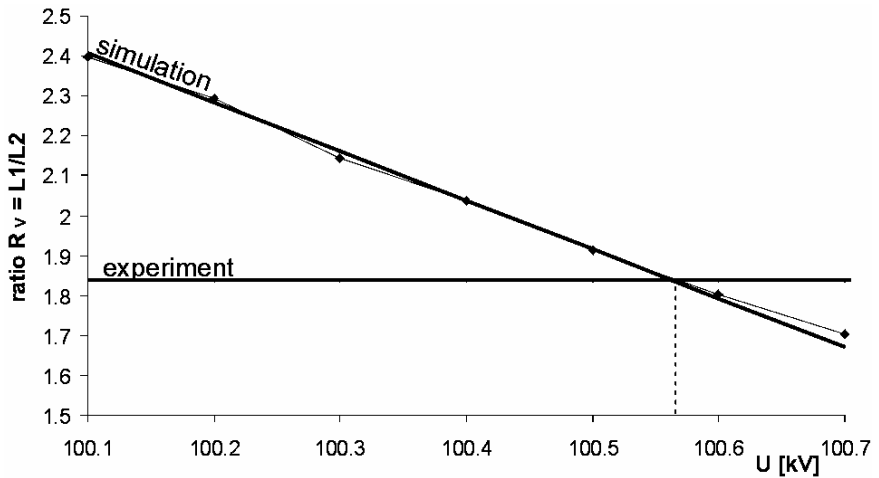


Fig. 5: Determination of the exact acceleration voltage at the day of the experiment by the intersection of the ratio R_v (horizontal line) obtained from the experimental patterns with the values measured from the dynamical simulated patterns.

In Fig. 5 the ratio $R_v=L_1/L_2$ (length indicated in Fig. 3b) of dynamically calculated CBED patterns is plotted. The horizontal line shows R_v determined from the experimental patterns. It can be seen, that the accelerating voltage on the day of the experiment was (100.57 ± 0.01) kV.

Lattice parameter of thin cubic stripes within 4H-SiC

In Fig. 6, the underlayed bright field image (see Fig. 2a) shows the electron probe position on the cubic stripe when taking the CBED patterns, marked by an encircled cross.

Overlaid on the BF image are the Kikuchi map and the experimental CBED pattern to demonstrate the relationship between the directions of the $[661]$ zone chosen for the CBED

analysis with respect to the $(1\bar{1}1)$ planes of the cubic stripe and to the (0001) planes of the specimen surface. In the experimental CBED pattern the indicated rectangular determines the region used for the lattice parameter determinations. In Fig. 7 an experimental CBED pattern is shown in (a) together with the corresponding scheme of the HOLZ-lines in (b) indicating the distances used for the ratio R_L . L_3 and L_4 , are formed by the indexed HOLZ line reflections, which were found to be sensitive to small lattice parameter changes. (The subscript number indicates the order of the reflection).

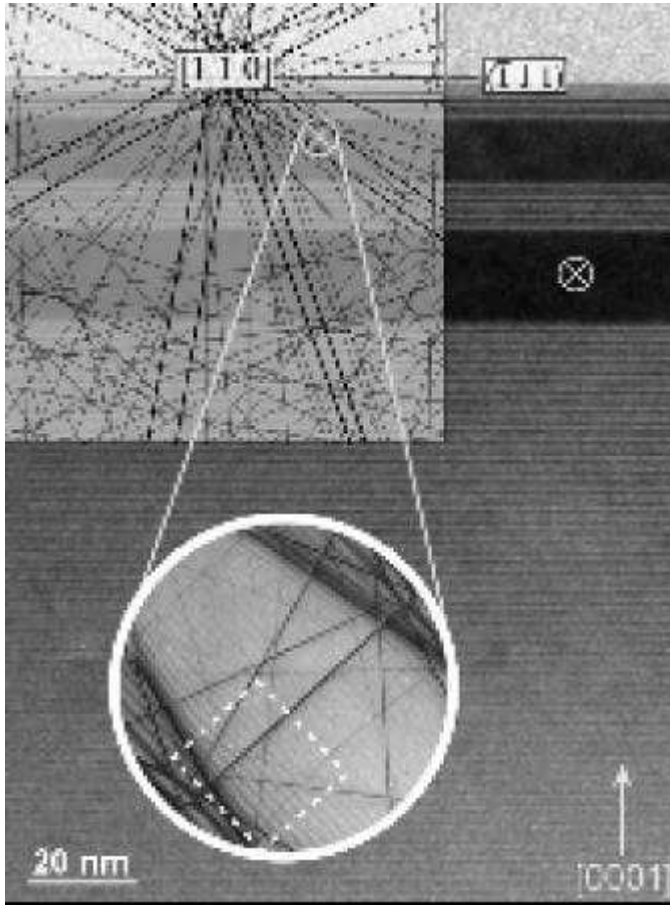


Fig. 6: Orientation relationship between the zone $[661]$ and the layer surface. The CBED pattern (the square marks the part of the pattern used for the lattice parameter determination) and the Kikuchi map are overlaid on the bright-field image. The position of the electron probe is indicated.

From the intersection between the ratios $R_L=L_3/L_4$ determined from the dynamically calculated CBED patterns for different a_{cub} -lattice parameter and the ratio $R_L=L_3/L_4$ determined from the experimental pattern, the lattice parameter has been determined to $a_{\text{stripe}}=(0.4362\pm 0.0001)$ nm. However when inspecting the experimental pattern carefully, obvious differences to the calculated patterns occur as demonstrated in Fig. 8. An asymmetry has been found in the experimental pattern, which is not present in the pattern seen in Fig. 8b, calculated for the case of the cubic symmetry with an $a=0.4362$ nm.

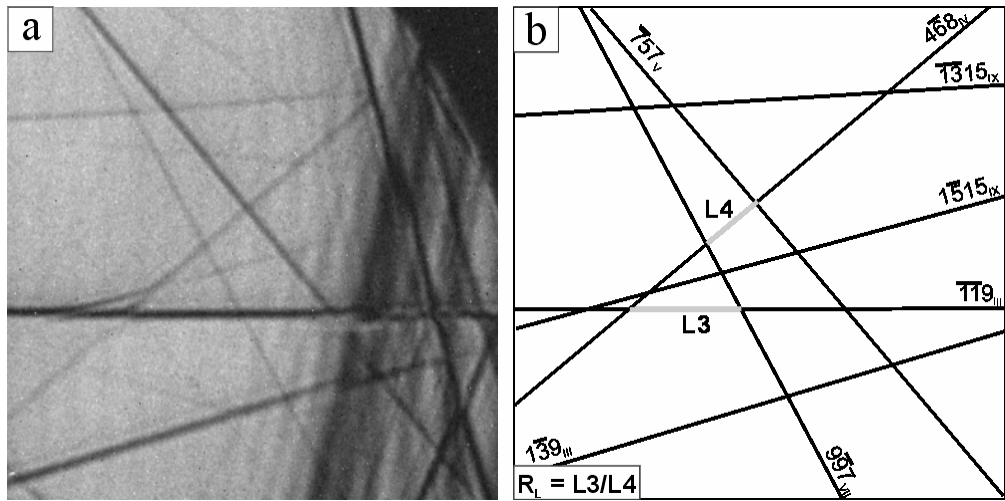


Fig. 7: The experimental [661] CBED pattern of 3C-SiC is shown in (a) together with the corresponding scheme of the HOLZ-lines in (b) indicating the distances used for the ratio R_L . L_3 and L_4 are formed by the indexed HOLZ line reflections (The subscript number indicates the order of the reflection.)

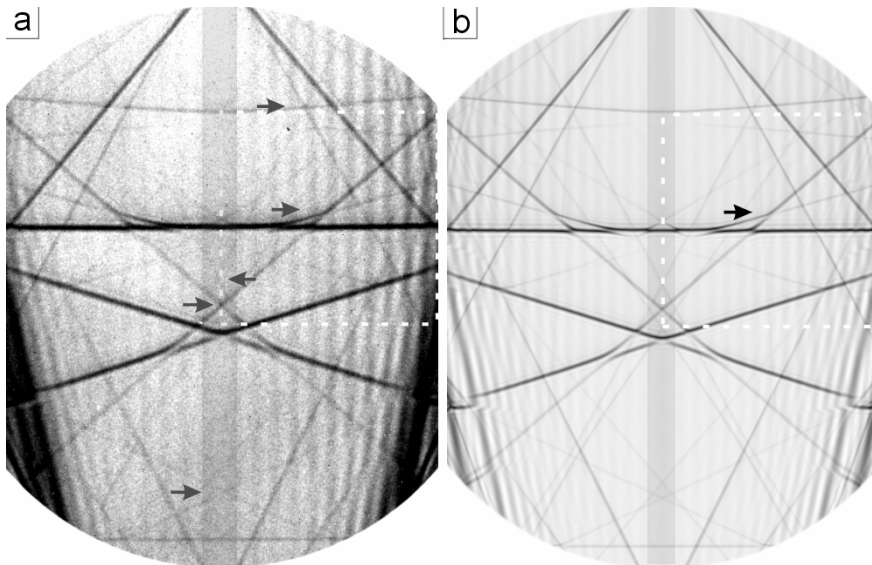


Fig. 8: (a) Experimental [661] SiC CBED pattern indicating the asymmetry along the inserted stripe. (b) Calculated cubic [661] SiC CBED pattern with $a=0.4362\text{nm}$, demonstrating the symmetry along the inserted white line. The arrows point to lines, where the difference between the two patterns can be recognized easily.

Very obvious distortions of the mirror symmetry along the perpendicular stripe inserted and changes in the lines are indicated by the arrows. As a distortion of the cubic symmetry may be reasonable due to the, however, small differences between the cubic and hexagonal SiC

polytypes (see Table 1), calculations were made for the case that the cubic symmetry F-43m is reduced to the rhombohedral R3m. [661] patterns were simulated with different a -values (0.4359nm, 0.4360nm, 0.4361nm, 0.4362nm) for the α -values (89.9°, 89.8°, 89.7°, 89.6°). The best fit between experiment and calculation was achieved at $a_{\text{stripe,rhom}}=0.4360\text{nm}$ and $\alpha_{\text{stripe,rhom}}=(89.78\pm 0.02)^\circ$ (Fig.9).

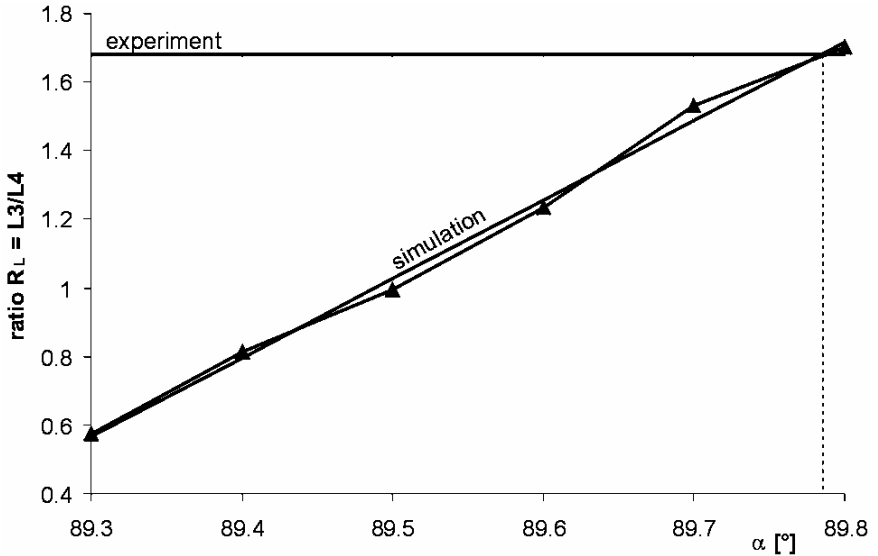


Fig. 9: The ratio $R_L=L_3/L_4$ determined from the dynamically calculated CBED patterns for rhombohedral (R3m) SiC plotted for $a=0.4360\text{nm}$ as a function of α_{rhom} . The horizontal line represents R_L for the experiment and from the line intersections $\alpha_{\text{rhom,stripe}}=(89.78\pm 0.02)^\circ$ was determined.

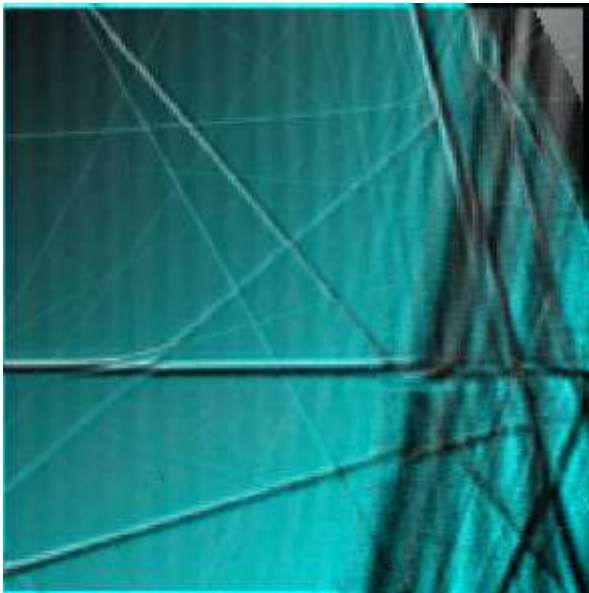


Fig. 10: Overlay of the experimental and calculated ($a=0.4360\text{nm}$, $\alpha=89.80^\circ$) patterns, visualizing a good fit.

A rhombohedral angle smaller than 90° at the tip of the rhombohedron with the [111] axis perpendicular to the (111) specimen surface may be a result of compressive strain on the cubic lattice due to the embedding in the hexagonal stripes. The corresponding a_{hex} -lattice parameter can be calculated resulting in an a -value of $a_{\text{stripe,hex}} = (0.3078 \pm 0.0001) \text{ nm}$. Compared to the a -lattice parameter of 4H-SiC determined by XRD for the bulk material (see Table 1) this value seems to be slightly too small. However the actual number of point defects may be the reason for small variations between the bulk SiC lattice parameters and the layer values. Using these values ($a = 0.4360 \text{ nm}$ and $\alpha = 89.78^\circ$), the asymmetry in the experimental pattern could be reproduced. As shown in the overlay of the simulated and the experimental pattern in Fig. 10, a qualitative good fit can already be seen by naked eyes.

This allows to conclude that the cubic stripe within 4H-SiC tends to grow pseudomorphically and for this reason it is rhombohedrally distorted. It moreover demonstrates the potential of the CBED method to determine such small strain states from a nanosized object.

Summary and Conclusion

SiC hetero-polytypic structures have been investigated by conventional and high resolution TEM and the lattice parameters of a thin cubic stripe have been determined by CBED. For the case of the stepped substrate, nearly free of defects, about 2nm thick cubic stripes are formed within the hexagonal layer. For the case of the growth on on-axis substrates, it was demonstrated that 6H/3C as well as 4H/3C stacks are formed on 6H and 4H-SiC substrates, respectively. By CBED the lattice parameters of the cubic stripe were determined to $a_{\text{hom}} = 0.4360 \text{ nm}$ $\alpha_{\text{hom}} = (89.78 \pm 0.02)^\circ$ demonstrating the rhombohedral distortion of the 3C stripes. It might be suggested that the result is valid also for the 2nm thick cubic stripes in the multi-quantum well structures grown on the stepped SiC substrate, although such layers are generally too thin for the lattice parameter determination by CBED.

Acknowledgements

The authors are grateful to Christian Zaubitzer for sample preparation and acknowledge the financial support of the Deutsche Forschungsgemeinschaft Sonderforschungsbereich 196.

References

- BECHSTEDT, F., KÄCKELL, X.: Phys. Rev. Lett. 75 (1995) 2180.
- CHUVILIN, A., KUPS, TH., KAISER, U.: "The Effect of the Signal-to-Noise-Ratio in CBED Patterns on the Accuracy of Lattice Parameter Determination", in preparation.
- DOYLE, P. A., TURNER, P. S.: Relativistic Hartree-Fock X-ray and Electron Scattering Factors Acta Cryst A24 (1968) 390.
- FISSEL, A., AKTARIEV, R., RICHTER, W.: Thin Solid Films 380 (2000) 42. (a)
- FISSEL, A., KAISER, U., PFENNIGHAUS, K., DUCKE, E., SCHRÖTER, B., RICHTER, W.: Inst. Phys. Conf. Ser. 142 (1996) 121. (b)
- FISSEL, A., KAISER, U., SCHRÖTER, B., RICHTER, W., BECHSTEDT, F.: Appl. Surface Science 184 (2001) 37. (c)
- FISSEL, A., SCHRÖTER, B., KAISER, U., RICHTER, W.: Appl. Phys. Lett. 77 (2000) 2418. (d)
- FISSEL, A.: About Heteropolytypic Structures: Molecular Beam Epitaxy, Characterization and Properties of Silicon Carbide, Habilitation FSU Jena 2002. (e)
- HOUGH, Pvc.: A method and means for recognizing complex patterns US Patent 3.069.654 (1962).

- KAISER, U., SAITOH, K., TSUDA, K., TANAKA, M.: Application of the CBED method for the determination of lattice parameters of cubic SiC films on 6H SiC substrates, *J. Electron Microsc.* 48(3) (1999) 221-233. (a)
- KAISER, U., CHUVILIN, A., RICHTER, W.: On the peculiarities of bright/dark contrast in HRTEM images of SiC polytypes et al *Ultramicroscopy*, **76** (1999) 21-37. (b)
- KRAEMER, S., MAYER, J., WITT, C., WEIKENMEIER, A., RUHLE, M.: Analysis of local strain in aluminium interconnects by energy filtered CBED, *Ultramicroscopy* 81 (2000) 245-262. (a)
- KRAEMER, S., MAYER, J.: Using the Hough transform for HOLZ line identification in convergent beam electron diffraction, *J. Microsc.* 194 (1999) 2-11. (b)
- KRÄUBLICH, J., BAUER, A., WUNDERLICH, B., GOETZ, K.: Lattice parameter measurements of 3C-SiC thin films grown on 6H-SiC(0001) substrate crystals, *Materials Science Forum* 335-356, 139 (2001).
- MORNIROLI, J. P.: *Diffraction Electronique En Faisceau Convergent A Grand Angle (LACBED)*, Societe Francaise des Microscopies, 1998, Paris.
- ROSSOUW, C. J., MILLER, P. R.: *Journal of Electron Microscopy* 849-864 (1999) 48.
- ROZEVELD, S. J., HOWE, J. M.: Determination of multiple lattice parameters from convergent-beam electron diffraction patterns, *Ultramicroscopy* 50 (1993) 41.
- TAKAGAHARA, T., TAKEDA, K.: *Phys. Rev. B* 46 (20) (1992) 16678.
- TSUDA, K., TANAKA, M.: Refinement of Crystal Structure Parameters using Convergent-Beam Electron Diffraction: The Low Temperature Phase of SrTiO₃, *Acta Cryst.* (1995) A51, 7-19.
- WAKAYAMA, Y., TAKAHASHI, Y., TANAKA, S.: Convergent beam electron diffraction measurement for local strain distribution in Si around NiSi₂ island, *Jpn. J. Appl. Phys.* 36 (1997) 5072-5078.
- WITTMAN, R., PARZINGER, C., GERTHEN, D.: Quantitative determination of lattice parameters from CBED patterns: accuracy and performance, *Ultramicroscopy* 70 (1998) 145-159..
- YONEMURA, M., SUEOKA, K., KAMEI, K.: Effect of heavy boron doping on the lattice strain around platelet oxide precipitates in Czochralski silicon wafers, *J. Appl Phys.* 88(1) (2000) 503-507.
- ZUO, J. M., SPENCE, J. C. H.: *Electron Microdiffraction*, Plenum Press New York (1992). (a)
- ZUO, J. M.: A new approach of the lattice parameter measurements using dynamic electron JEM 47(2), 121-127 (1998). (b)